
Postexercise Lung Uptake of ^{99m}Tc -Sestamibi Determined by a New Automatic Technique: Validation and Application in Detection of Severe and Extensive Coronary Artery Disease and Reduced Left Ventricular Function

Claudia Bacher-Stier, Tali Sharir, Paul B. Kavanagh, Howard C. Lewin, John D. Friedman, Romalisa Miranda, Guido Germano, and Daniel S. Berman

Departments of Imaging and Medicine and Burns and Allen Research Institute, Cedars-Sinai Medical Center, Los Angeles; and Department of Medicine, School of Medicine, University of California, Los Angeles, Los Angeles, California

This study validated a new automatic algorithm for assessment of lung-to-heart ratio (L/H) of radiotracers in myocardial perfusion SPECT and assessed the diagnostic value of ^{99m}Tc -sestamibi L/H after exercise. **Methods:** The new technique extracts a left ventricular region of interest (ROI) from a summed anterior projection image and generates a lung ROI by reshaping and translating the left ventricular ROI. This algorithm was applied to 230 patients who underwent exercise ^{99m}Tc -sestamibi SPECT (gated SPECT, $n = 88$) with first-pass ventriculography. Normal values were established in 26 patients in whom the likelihood of coronary artery disease (CAD) was 5% or less. An abnormality threshold for detecting severe and extensive CAD was defined in a subgroup of 109 patients who underwent coronary angiography and was validated in a prospective group ($n = 72$). **Results:** The success rate of the automatic algorithm was 97%. Excellent correlation was found between automatic and manual L/H values ($r = 0.95$; $P < 0.001$). The mean L/H was higher in patients with a peak exercise ejection fraction (EF) less than 40% versus 40% or more (0.51 ± 0.07 versus 0.43 ± 0.05 , $P < 0.001$) and in patients with a poststress EF less than 40% versus 40% or more (0.50 ± 0.07 versus 0.44 ± 0.06 , $P < 0.01$). A threshold of L/H greater than 0.44 yielded a sensitivity and specificity of 63% and 81%, respectively, for identifying severe and extensive CAD in the prospective group and a sensitivity of 86% in identifying stenosis of 90% or more in the proximal left anterior descending artery. **Conclusion:** The new automatic algorithm for assessing L/H correlated well with manually derived L/H for ^{99m}Tc -sestamibi as well as ^{201}Tl SPECT. An increased postexercise ^{99m}Tc -sestamibi L/H adds significant diagnostic value to study myocardial perfusion SPECT as a marker of severe and extensive CAD and reduced ventricular function.

Key Words: ^{99m}Tc -sestamibi; lung uptake; automatic technique; coronary artery disease; left ventricular function

J Nucl Med 2000; 41:1190–1197

Increased lung uptake of ^{201}Tl after exercise (1,2), as well as after pharmacologic stress (3), has been shown to correlate with the presence of severe coronary artery disease (CAD) (3,4), the extent and severity of scintigraphic perfusion defects (3,5), and left ventricular dysfunction (6–9). Because of its physical and biologic properties, ^{99m}Tc -sestamibi is now more commonly used than ^{201}Tl for myocardial perfusion imaging. Only a few studies, based on highly selected patient populations (10–12), have evaluated the diagnostic value of ^{99m}Tc -sestamibi lung uptake. Furthermore, previously described algorithms for determining lung-to-heart ratio (L/H) have required various degrees of operator interaction during processing (10–13), and a completely automatic method for determination of abnormal lung uptake has not been defined for either ^{201}Tl or ^{99m}Tc -sestamibi. We have developed a fully automatic approach for calculating the L/H of radiotracers. The new technique extracts a left ventricular region of interest (ROI) from a summed anterior projection image using heuristics and mathematic operators and generates a lung ROI by reshaping and translating the left ventricular ROI. This study was undertaken to describe and validate the new automatic algorithm and to assess the diagnostic value of ^{99m}Tc -sestamibi L/H uptake after exercise.

MATERIALS AND METHODS

Study Population

Two hundred thirty patients who underwent separate-acquisition dual-isotope resting ^{201}Tl and exercise ^{99m}Tc -sestamibi myocardial perfusion SPECT (14) were evaluated for the L/H of ^{99m}Tc -sestamibi uptake after exercise. The automatic assessment of L/H was successful in 223 of the initial patients (97%). The program failed in 7 patients because of high gut activity, leading to incorrect ROI placement. The final study population, comprising 223 patients, was divided into the following 3 subgroups (Table 1).

Received Jun. 24, 1999; revision accepted Nov. 1, 1999.

For correspondence or reprints contact: Daniel S. Berman, MD, Cedars-Sinai Medical Center, 8700 Beverly Blvd., Rm. A041, Los Angeles, CA 90048.

TABLE 1
Patient Characteristics and Exercise Variables

Variable	Group 1 (n = 26)	Group 2 (n = 125)	Group 2A (n = 109)	Group 3 (n = 72)
Age (y)	50 ± 12.3	65 ± 11.3*	65 ± 11.2*	68 ± 11.2*
No. of men	14 (54)	97 (78)†	83 (76)‡	58 (81)†
History of MI	0	34 (27)*	24 (22)*	26 (36)*
Angina§	0	54 (43)*	39 (36)*	26 (36)*
ST depression§	1 (4)	74 (59)*	69 (63)*	39 (54)*
FP EF	67 ± 7.4	53 ± 13.3*	56 ± 10.4*	56 ± 14.4*
GS EF (n = 181)	64 ± 6.4 (n = 26)	54 ± 15.4* (n = 88)	56 ± 13.4* (n = 73)	51 ± 12* (n = 67)

**P* < 0.001 vs. group 1.

†*P* < 0.01 vs. group 1.

‡*P* = 0.02.

§During exercise.

MI = myocardial infarction; FP = first-pass radionuclide ventriculography; EF = ejection fraction; GS = gated SPECT.

Numbers in parentheses are percentages.

Normal Limits (Group 1). Twenty-six patients with a low likelihood of CAD (<5%), determined by CADENZA (15) (a classification based on age, sex, risk factors, symptoms, and exercise electrocardiography) and normal myocardial perfusion SPECT, were evaluated to establish normal values for ^{99m}Tc-sestamibi L/H after exercise.

Criterion for Abnormality (Group 2). This group consisted of 125 patients referred for evaluation of CAD. Patients with prior coronary bypass grafting or nonischemic heart disease were excluded. One hundred nine of these patients (group 2A) had coronary angiography within 60 d of the myocardial perfusion testing. The optimal threshold for ^{99m}Tc-sestamibi L/H for detection of severe and extensive (S+E) CAD was determined in this subgroup by analysis of receiver operating characteristics.

Prospective Validation (Group 3). The threshold for abnormality of ^{99m}Tc-sestamibi L/H was tested in an additional group of 72 consecutive prospectively analyzed patients who underwent coronary angiography within 90 d of nuclear testing and had no intervening revascularization procedure.

Exercise and Imaging Protocol

All patients were withdrawn from β-blocking drugs and long-acting nitrates for 48 and 24 h, respectively, before nuclear testing. SPECT images were acquired at rest after an injection of 111–167 MBq ²⁰¹Tl. All patients then underwent symptom-limited treadmill testing (Bruce protocol), achieving at least 85% of the age-predicted maximal heart rate. Electrocardiographic response was considered positive when horizontal or downsloping ST-segment depression of 1 mm or upsloping ST-segment depression of 1.5 mm was observed. The response was considered nondiagnostic when nonspecific ST-T wave abnormalities were present at baseline electrocardiography. A bolus of 925–1480 MBq ^{99m}Tc-sestamibi was injected at peak stress, and first-pass radionuclide ventriculography was performed in the anterior view (16). Exercise was continued at the same level for 60 s and at 1 stage lower for an additional 2 min. SPECT was started 15–30 min later. As shown in Table 1, 181 of the 223 patients (81%) also underwent gated SPECT.

Acquisition Protocol

SPECT images were acquired with either a dual-head camera (Vertex; ADAC Laboratories, Milpitas, CA) using continuous step-and-shoot detector rotation or a triple-head camera (Prism 3000; Picker International, Cleveland, OH) using continuous detector rotation, obtaining 60 projections over a 180° circular orbit (45° right anterior oblique to left posterior oblique). Both cameras were equipped with a high-resolution collimator. Resting ²⁰¹Tl images were acquired with a 30% window over the 68- to 80-keV photopeak and a 20% window over the 167-keV photopeak. Stress ^{99m}Tc-sestamibi used a 15% window over the 140-keV photopeak. Gated acquisition of ^{99m}Tc-sestamibi used 8 frames per cardiac cycle, with a 100% symmetric acceptance window (17). Acquisition times were 20 and 15 min for the resting ²⁰¹Tl and gated ^{99m}Tc-sestamibi, respectively. The gated projection datasets were prefiltered with a 2-dimensional Butterworth filter (order 5, critical frequency of 0.25 cycles per pixel, pixel size of 0.64 cm for the Vertex camera and 0.53 cm for the Prism camera). The summed projection datasets were filtered with a Butterworth filter (order 5, critical frequency of 0.33 cycles per pixel) and reconstructed with filtered backprojection (ramp filter).

First-pass data were acquired with a mobile multicrystal gamma camera (Sim-400; Scintacor, Inc., Milwaukee, WI) (18) equipped with a high-sensitivity collimator, using the following acquisition parameters: a 50% window over the 140-keV ^{99m}Tc energy peak, 40 frames per second, and 25 ms per frame. Motion correction of the first-pass data was applied using an ²¹⁴Am point source (19).

Image Analysis

Semiquantitative visual interpretation of myocardial perfusion SPECT images was performed using short-axis and vertical long-axis slices divided into 20 segments (20). These segments were assigned on 6 evenly spaced regions in the apical, midventricular, and basal slices of the short-axis views and 2 apical segments on a midventricular long-axis slice. A 5-point scoring scale for tracer uptake was used, in which 0 was normal uptake, 1 was mildly reduced uptake, 2 was moderately reduced uptake, 3 was severely reduced uptake, and 4 was no uptake. Summed stress and rest scores were calculated as the sums of scores of the 20 segments in the stress and rest images, respectively. The sum of the differences between each of the 20 segments on the stress and rest images was defined as the summed difference score (20).

Ejection Fraction, End-Diastolic Volume, and Transient Ischemic Dilation

The relationship between the L/H of ^{99m}Tc-sestamibi and left ventricular ejection fraction (EF) by first-pass and gated SPECT was determined for group 2 patients. First-pass EF was calculated semiautomatically after creation of a final representative heart cycle, definition of end-diastolic and end-systolic regions of interest (ROIs), and background modification, as previously reported (16,19). For gated SPECT, the transaxial gated SPECT image sets were automatically reoriented into short-axis sets and processed using the quantitative gated SPECT algorithm for the assessment of left ventricular EF and end-diastolic volume (17).

The transient ischemic dilation ratio (TID) was determined as the ratio of ungated poststress ventricular volume to the ungated resting volume (21). We previously showed that a TID of 1.22 or more was related to the presence of S+E CAD (21); therefore, this threshold was used to dichotomize the study group for further evaluation.

Assessment of Lung Uptake

The anterior view of the SPECT projection dataset was automatically identified and summed to 4 adjacent projections (2 on either side) to increase count statistics. The algorithm then automatically identified the myocardial borders by convolving the projection image with a feature detector consisting of the double derivative of a 2-dimensional gaussian curve with iteratively varied SD, in a manner similar to that reported by our group (22). Four different ROIs were automatically generated (Fig. 1), 2 over the heart and 2 over the lung field: Heart_{AVG} was the ROI encircling the whole myocardium; Heart_{MAX} was a 4 × 4 pixel ROI containing the hottest pixel within the myocardium; Lung_{AVG} was a crescent-shaped ROI 3 pixels away from the heart, generated by truncation and translation of the Heart_{AVG} ROI and positioned over the middle of the left lung; and Lung_{MAX} was a 4 × 4 pixel ROI containing the hottest pixel within Lung_{AVG}. The average value for counts per pixel was calculated for each ROI and used for calculating 3 different values of L/H: Lung_{AVG}/Heart_{AVG}, Lung_{AVG}/Heart_{MAX}, and Lung_{MAX}/Heart_{MAX}. These automatic L/H values were validated by correlation with the respective manual L/H values obtained by operator definition of the lung and heart ROIs, with the operator unaware of the ROIs generated by the automatic program and the clinical data. Manual L/H values were determined for each patient on 2 occasions, and the mean of these 2 measurements was considered the gold standard for the respective automatic L/H.

The automatic algorithm was also applied to the resting ²⁰¹Tl studies of patient groups 1 and 2 and worked successfully in 23 of the 26 patients (88%) in group 1 and in 113 of the 125 patients (90%) in group 2. Automatically derived L/H values for ²⁰¹Tl were also compared with manual L/H values using the method described for ^{99m}Tc-sestamibi.

Coronary Angiography

Insignificant CAD was defined as stenosis of less than 70% in all vessels. Mild to moderate CAD was defined as stenosis of at least 70% but less than 90% in 1 or more vessels, or stenosis of at least 90% in 1 vessel other than the proximal left anterior descending coronary artery (LAD). S+E CAD was defined as stenosis of at least 90% in the proximal LAD (S+E LAD) or stenosis of at least 90% in 2 or 3 coronary arteries (S+E 2/3 CAD) (21).

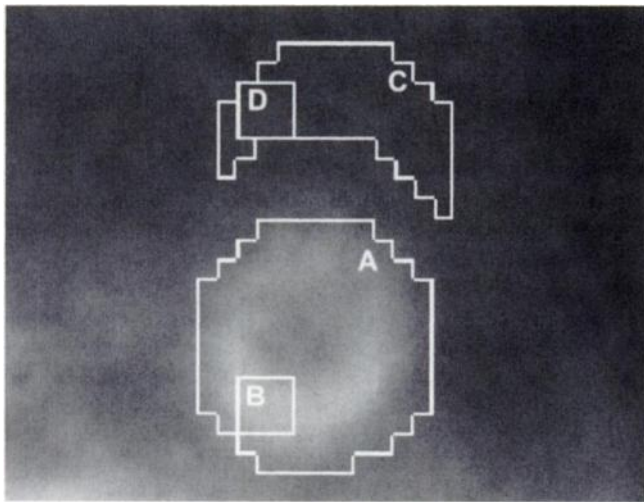


FIGURE 1. Regions of interest in left lung and heart for calculation of Heart_{AVG} (A), Heart_{MAX} (B), Lung_{AVG} (C), and Lung_{MAX} (D) L/H values.

Statistical Analysis

Data are presented as mean ± SD. Patient groups were compared using the χ^2 test for categorical variables and the unpaired Student *t* test for continuous variables. $P < 0.05$ was considered statistically significant. Linear regression analysis was performed for correlation between the manual and the automatic methods. The threshold for L/H abnormality was determined by applying receiver operating characteristic analysis to group 2 patients, using S+E CAD as a gold standard.

RESULTS

Table 1 summarizes patient characteristics and exercise variables. The patients in groups 2 and 3 were older, with a higher proportion of men, and had a higher incidence of exercise-induced angina and ST depression compared with group 1. EFs by first-pass and gated SPECT were significantly lower in groups 2 and 3 than in group 1.

Validation of Automatic L/H

The automatic and manual L/H values of ^{99m}Tc-sestamibi correlated linearly over a wide range for all 3 methods of calculating automatic L/H: high correlation coefficients were observed for Lung_{AVG}/Heart_{AVG} ($y = 1.01x - 0.006$; $r = 0.95$) as well as for Lung_{AVG}/Heart_{MAX} ($y = 0.87x + 0.05$; $r = 0.83$) and Lung_{MAX}/Heart_{MAX} ($y = 0.84x + 0.06$; $r = 0.91$).

Because the highest correlation coefficient was obtained for Lung_{AVG}/Heart_{AVG} ($P \leq 0.001$), this method was chosen for further assessment of the clinical value of the L/H. Automatically and manually derived L/H values of ²⁰¹Tl also showed highly significant linear correlation ($r = 0.93$; $P < 0.001$) (Fig. 2).

Identification of S+E CAD

Threshold for Abnormality. The mean L/H of postexercise ^{99m}Tc-sestamibi in patients with a low likelihood of CAD (group 1) was 0.40 ± 0.03 . Receiver operating characteristic analysis in group 2A for identifying S+E CAD yielded an area of 0.78 under the curve relating the true-positive rate to 1 minus the true-negative rate (Fig. 3), which was significantly different from 0.5 ($P < 0.001$). The optimal L/H threshold for abnormality was 0.44 (1.3 SD above the mean L/H of the low-likelihood group). This threshold yielded a sensitivity of 71% (32/45) and a specificity of 75% (49/65) in identifying combined S+E CAD.

The relationship between L/H and angiographic results in group 2A is displayed in Figure 4. The mean L/H was 0.49 ± 0.07 in patients with S+E LAD ($n = 21$) and 0.45 ± 0.05 in patients with S+E 2/3 CAD ($n = 24$), compared with 0.40 ± 0.03 in the low-likelihood group ($P < 0.01$). One of 26 patients in the low-likelihood group had an elevated L/H (>0.44). The mean L/H was 0.41 ± 0.06 in patients with insignificant CAD, and 7 of 22 had an increased L/H. The mean L/H was 0.41 ± 0.04 in patients with mild to moderate CAD, and 8 of 42 showed an elevated L/H (insignificant P versus the low-likelihood group). The L/H was abnormal (>0.44) in 17 of 21 patients (81%) with S+E LAD and in 15 of 24 patients (63%) with S+E 2/3 CAD. The specificity for identifying S+E LAD disease was 65% (58/89).

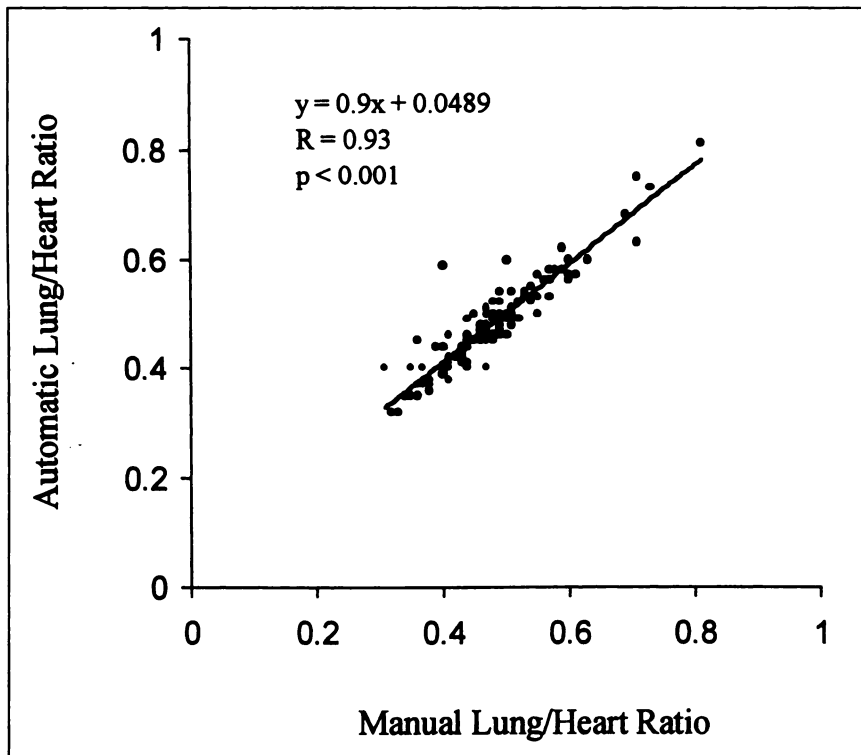


FIGURE 2. Correlation between automatically and manually derived L/H of ^{201}Tl .

Validation of Threshold for Abnormality. Based on the threshold for L/H abnormality (>0.44) defined in group 2A, overall sensitivity and specificity in identification of S+E CAD were 63% (22/35) and 81% (29/36), respectively, in the prospective group (group 3). Figure 5 shows the relationship between L/H and angiographic results for that group. The sensitivity for identifying S+E LAD was 87% (13/15), and the sensitivity for identifying S+E 2/3 CAD was only 45% (9/20). The specificity for S+E LAD stenosis was 71% (40/56). Mean L/H was 0.47 ± 0.02 in patients with S+E

LAD and 0.46 ± 0.06 in patients with S+E 2/3 CAD ($P < 0.01$ versus 0.40 ± 0.03 in the low-likelihood group). The mean L/H was 0.39 ± 0.05 in patients without S+E CAD ($n = 36$) (insignificant P versus the low-likelihood group).

Relationship Between L/H and Other Markers of S+E Coronary Disease

L/H and Summed Stress Score. Figure 6 displays the relationship between the automatically derived L/H of $^{99\text{m}}\text{Tc}$ -sestamibi uptake and the extent and severity of

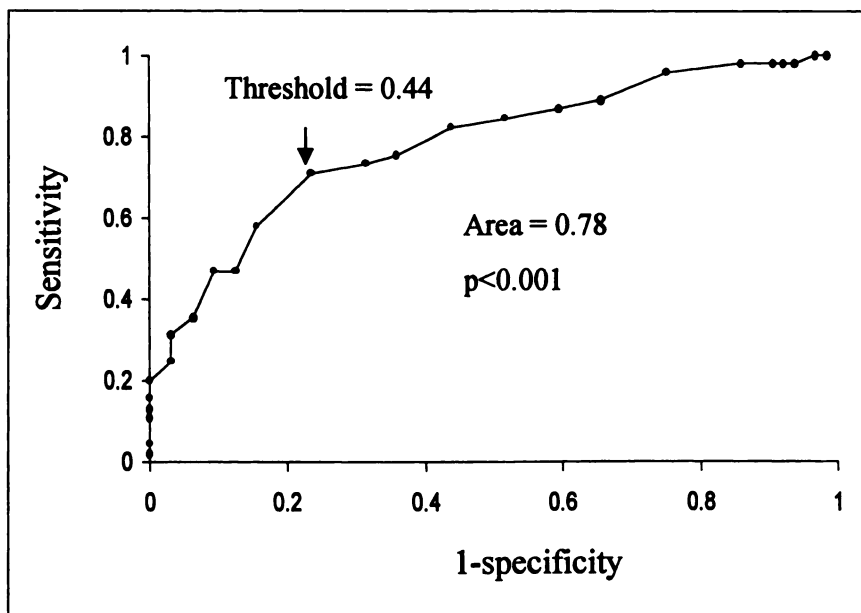


FIGURE 3. Receiver operating characteristic analysis for determining optimal threshold for L/H for detection of S+E CAD in group 2A patients. Point of optimal threshold is indicated by arrow.

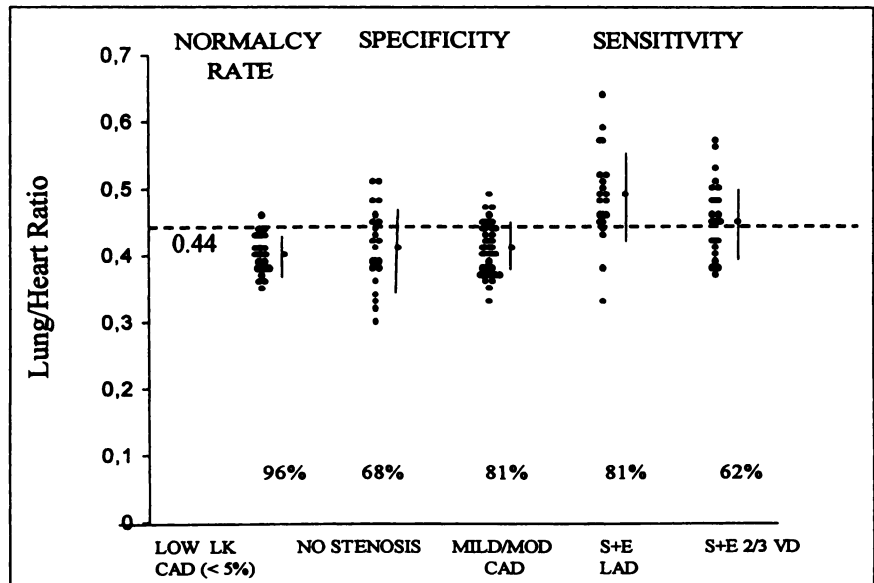


FIGURE 4. Relationship between L/H and presence and S+E of CAD in group 2A patients. Mean \pm SD values are shown at right of individual values of each group. Dashed line is upper normal limit for L/H. LK = likelihood; MOD = moderate; VD = vessel disease.

perfusion defects, measured as the summed stress score in group 2A. The frequency of elevated L/H (>0.44) increased progressively with the summed stress score. Patients with a summed stress score > 13 had a significantly higher frequency of elevated L/H than did patients with normal perfusion (summed stress score < 4).

L/H and TID. Forty-seven of 109 patients (43.1%) of group 2A had an elevated L/H, and 20 of 109 (18.3%) had an abnormal TID (≥ 1.22). Patients with an increased TID had a higher L/H than did those with a normal TID (< 1.22) (0.53 ± 0.04 versus 0.41 ± 0.04 , $P = 0.001$). Five of 6 patients (83.3%) with a normal TID but an elevated L/H had S+E CAD. Of 2 patients who had an abnormal TID but a normal L/H, neither had S+E CAD.

Correlation with EF and End-Diastolic Volume

A fair but significant inverse correlation was observed between L/H and peak exercise EF measured by first-pass

SPECT and between L/H and poststress EF measured by gated SPECT ($r_s = -0.50$ and -0.47 , respectively; $P < 0.001$). The L/H was significantly higher in patients with an EF less than 40% than in patients with an EF greater than 40% both at peak stress and after stress (Table 2). Applying the L/H cutoff of 0.44 yielded a sensitivity and specificity of 91% and 61%, respectively, in detecting a peak-stress first-pass EF less than 40% and a sensitivity and specificity of 88% and 63%, respectively, in detecting a poststress gated EF less than 40%. The poststress end-diastolic volume, derived from gated SPECT, was significantly higher in patients with an L/H greater than 0.44 than in patients with an L/H of 0.44 or less (121 ± 55.6 mL versus 90 ± 33 mL, $P = 0.008$).

Relationship Between L/H and Clinical Variables

Table 3 summarizes the relationship between clinical variables and L/H. Patients with an L/H greater than 0.44

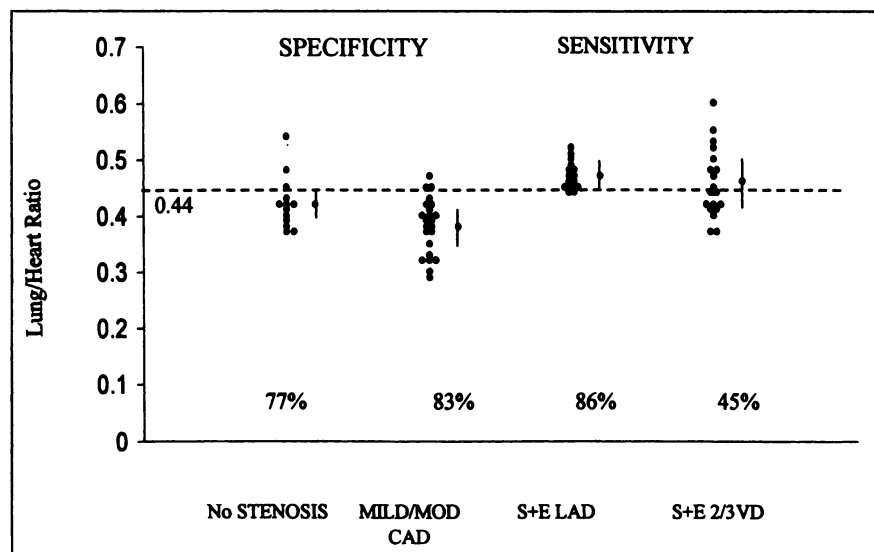


FIGURE 5. Relationship between L/H and presence and S+E of CAD in group 3 patients (validation group). Mean \pm SD values are shown at right of individual values of each group. Dashed line is upper normal limit for L/H. MOD = moderate; VD = vessel disease.

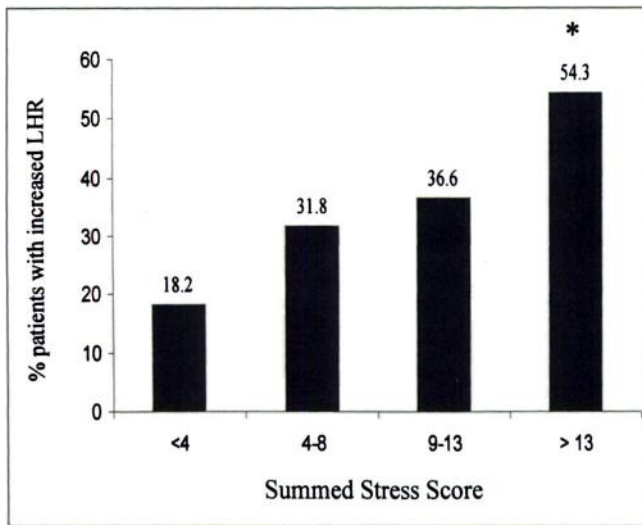


FIGURE 6. Percentage of patients with increased L/H according to summed stress score (summed stress score ≤ 4 , 2/11; 4-8, 7/22; 9-13, 11/13; ≥ 13 , 25/46). * $P < 0.05$; LHR = L/H.

had a higher frequency of prior myocardial infarction (35% versus 22%, $P = 0.005$) and diabetes mellitus (15% versus 8%, $P = 0.04$). No significant differences existed in age; sex; weight; history of smoking or hypertension; and maximal heart rate, chest pain and ST segment depression during exercise between patients with an L/H greater than 0.44 and an L/H of 0.44 or less.

DISCUSSION

This study validated a newly developed automatic algorithm for assessment of L/H from myocardial perfusion SPECT and determined the diagnostic value of postexercise ^{99m}Tc -sestamibi lung uptake.

Validation of Automatic L/H in SPECT

To our knowledge, all previously reported approaches for assessment of lung uptake of ^{201}Tl or ^{99m}Tc -sestamibi have been either manual (2,4,10,12,13,23) or semiautomatic, with the operator assisting ROI generation (13). Our newly developed algorithm does not require operator interaction, although a manual ROI definition feature is provided for cases in which the algorithm does not correctly identify the

TABLE 2
Relationship Between L/H and EF in Group 2 Patients (n = 125)

	EF (%)	n	L/H
Peak exercise FP EF	<40	22	0.51 \pm 0.07*
	≥ 40	103	0.43 \pm 0.05
Postexercise GS EF	<40	16	0.50 \pm 0.07†
	≥ 40	72	0.44 \pm 0.06

* $P < 0.001$ vs. EF $\geq 40\%$.
† $P < 0.01$ vs. EF $\geq 40\%$.
FP = first-pass ventriculography; GS = gated SPECT.

TABLE 3
Relationship Between L/H and Clinical Variables in Group 2 Patients (n = 125)

Variable	Normal L/H (≤ 0.44) (n = 65)	Elevated L/H (> 0.44) (n = 60)	P
Age (y)	66 \pm 12	65 \pm 11	NS
No. of men	48 (74)	49 (82)	NS
Weight (kg)	76.1 \pm 14.5	79.3 \pm 11	NS
Smoking	8 (12)	7 (12)	NS
Hypertension	40 (62)	29 (48)	NS
Diabetes mellitus	5 (8)	9 (15)	0.04
Prior myocardial infarction	14 (22)	21 (35)	0.005
Maximal heart rate during exercise	141 \pm 15	138 \pm 16	NS
Chest pain during exercise	31 (48)	23 (38)	NS
ST depression during exercise	42 (64)	35 (58)	NS

NS = nonsignificant.
Numbers in parentheses are percentages.

heart and lungs. The success rate was high for both ^{99m}Tc -sestamibi and ^{201}Tl (97% and 90%, respectively). The algorithm executes in less than 10 s on a SPARC 10 computer (Sun Microsystems, Inc., Mountain View, CA), and its fully automated approach saves technologist time and eliminates observer variability. The feasibility of L/H measurement from the sum of myocardial perfusion projection images adjacent to the anterior projection has been discussed (4,8,9,24). The anterior projection images were selected for this study because spatial separation of heart and lung ROIs is best along this direction (2). Despite a lower count density, an excellent correlation between L/H derived from unprocessed projection frames acquired for SPECT and L/H derived from standard planar imaging has been reported by several authors for ^{201}Tl (2,25,26).

This study showed an excellent linear correlation between automatic and manual L/H for ^{99m}Tc -sestamibi and ^{201}Tl , particularly for Lung_{AVG}/Heart_{AVG}. Thus, the automatic algorithm may be applied successfully with both tracers.

Clinical Evaluation

Although some have suggested that the additional diagnostic value of an increased ^{201}Tl L/H is lost when using ^{99m}Tc -sestamibi (7,27), no conclusive results exist concerning the clinical usefulness of an increased ^{99m}Tc -sestamibi L/H. This lack may be caused by the highly selected patient populations and small numbers of patients in which ^{99m}Tc -sestamibi L/H has been evaluated (10), the late starting times of acquisitions (10,27), or the methods used for drawing ROIs and calculating L/H. We know of only 1 study that sought to determine the value of an elevated L/H in a large patient cohort (12); however, L/H calculation was performed directly on the tomographic short-axis cross section, a method that has previously been shown, with ^{201}Tl , to be inferior to L/H assessment from planar as well as projection images (9).

Normal Limits and Cutoff for ^{99m}Tc -Sestamibi L/H

Mean L/H values for ^{99m}Tc -sestamibi in this study (0.40 ± 0.03), as well as others (10,12), were slightly higher than L/H values reported for ^{201}Tl (ranging from 0.24 to 0.28 (2,9)). The abnormality cutoff value, which, in our study, was defined for ^{99m}Tc -sestamibi L/H (>0.44), was quite comparable with the established threshold for ^{201}Tl (0.45–0.50) (4,6,7,25). Thus, the difference between normal and abnormal values seems to be smaller for ^{99m}Tc -sestamibi than for ^{201}Tl .

^{99m}Tc -Sestamibi L/H for Identifying S+E CAD

In 2 previous studies, an increased L/H with ^{99m}Tc -sestamibi was reported to have either limited (10) or no diagnostic value (27). However, in those studies imaging was started 60–120 min after tracer application (10,27). Although Giubbini et al. (10) found an inverse correlation between L/H and left ventricular function, they did not find a relationship with the severity or extent of CAD. An impact from the starting time of the acquisition has been suggested by Hurwitz et al. (12), who were able to show a good correlation between L/H and angiographic findings on immediate images (4 min after stress) but not on delayed images. L/H on late images correlated with left ventricular dysfunction (12) but not with CAD. Thus, early imaging may be necessary for applying L/H calculation to identify S+E CAD with ^{99m}Tc -sestamibi (10,11), implying that some lung washout, as occurs with ^{201}Tl , may also occur with ^{99m}Tc -sestamibi (2,28).

Our acquisition used early imaging, beginning 15–20 min after exercise. We identified patients with S+E CAD, with fair to good overall sensitivity (63% in the pilot group and 71% in the validation group, respectively), along with high overall specificity (77% in the pilot group and 80% in the validation group, respectively). Detection of severe proximal LAD disease by an elevated L/H also had high sensitivity and specificity (86% and 73%, respectively), in accordance with a recent report (12). A similar role for L/H in identifying severe LAD disease has been shown with ^{201}Tl (23,29,30). On the basis of our results, we recommend early imaging (15–20 min) with ^{99m}Tc -sestamibi to optimize the value of the L/H as a predictor of S+E CAD. The correlation between L/H and 2 other markers of S+E CAD—the TID (21) and a summed stress score greater than 13—supports the assumption that an elevated L/H can be regarded as a marker for S+E CAD.

L/H and TID

The sensitivity of an elevated L/H for identifying S+E LAD disease was higher in this study (86%) than that previously reported for an abnormal TID (70%) (21). Five of 6 patients with an elevated L/H without TID had S+E CAD, suggesting the L/H to have a slightly higher predictive value than does the TID for detection of S+E CAD. However, larger studies designed to compare the value of an increased ^{99m}Tc -sestamibi L/H with the value of TID would be of great interest. A recent report showed that only a weak relation-

ship exists between TID and the ^{201}Tl L/H (31). That report further observed that characteristics differed between patients with an elevated L/H and patients with an abnormal TID and concluded that the mechanisms producing TID and increased lung uptake were likely to be different.

^{99m}Tc -Sestamibi L/H and Left Ventricular Function

We found a fair but significant inverse linear relationship, similar to what was reported by others, between L/H and left ventricular EF at peak exercise (10). A correlation between left ventricular EF at peak exercise and L/H was described for ^{201}Tl (7); however, other reports failed to show a relationship between increased ^{201}Tl lung uptake and resting EF (2,8,25). Johnson et al. (32), using ^{99m}Tc -sestamibi gated SPECT in ischemic patients, showed that EF early after exercise was frequently lower than resting EF. This difference in EFs may explain why the patients in our study, using poststress ^{99m}Tc -sestamibi, showed a significant inverse correlation between L/H and EF that was not seen previously with resting ^{201}Tl .

^{99m}Tc -Sestamibi L/H and Clinical Parameters

We found no correlation between L/H and most clinical variables, i.e., age, maximal heart rate, patient weight, arterial hypertension, β -blocker or digoxin therapy, and smoking. For ^{201}Tl L/H, however, some authors have found a relationship with parameters such as maximal heart rate (6), patient weight (6), and angina and ST depression during exercise (4). We found that only in patients who had myocardial infarction or diabetes were L/H values more frequently elevated; this finding partly accords with previous findings for ^{201}Tl (4,5,25).

CONCLUSION

We have developed a fully automatic method for determining the L/H of ^{99m}Tc -sestamibi or ^{201}Tl uptake. An elevated L/H with ^{99m}Tc -sestamibi, similar to ^{201}Tl , appears to be a marker of S+E CAD, especially when imaging occurs early after exercise. Although the ^{201}Tl L/H has been shown to predict cardiac events (33), the prognostic impact of an increased ^{99m}Tc -sestamibi lung uptake remains to be assessed.

ACKNOWLEDGMENT

This study was presented in part at the 45th annual meeting of the Society of Nuclear Medicine, Toronto, Ontario, Canada, June 1998.

REFERENCES

1. Kahn JK, Carry MM, McGhie I, Pippin JJ, Akers MS, Corbett JR. Quantitation of postexercise lung thallium-201 uptake during single photon emission computed tomography. *J Nucl Med.* 1989;30:288–294.
2. Aksut SV, Mallavarapu C, Russell J, Heo J, Iskandrian AS. Implications of increased lung thallium uptake during exercise single photon emission computed tomography imaging. *Am Heart J.* 1995;130:367–373.
3. Iskandrian AS, Heo J, Nguyen T, Lyons E, Paugh E. Left ventricular dilatation and pulmonary thallium uptake after single-photon emission computer tomography using thallium-201 during adenosine-induced coronary hyperemia. *Am J Cardiol.* 1990;66:807–811.

4. Hurwitz GA, O'Donoghue JP, Powe JE, Gravelle DR, MacDonald AC, Finnie KJ. Pulmonary thallium-201 uptake following dipyridamole-exercise combination compared with single modality stress testing. *Am J Cardiol.* 1992;69:320-326.
5. Villanueva FS, Kaul S, Smith WH, Watson DD, Varma SK, Beller GA. Prevalence and correlates of increased lung/heart ratio of thallium-201 during dipyridamole stress imaging for suspected coronary artery disease. *Am J Cardiol.* 1990;66:1324-1328.
6. Jain D, Thompson B, Wackers FJ, Zaret BL. Relevance of increased lung thallium uptake on stress imaging in patients with unstable angina and non-Q wave myocardial infarction: results of the Thrombolysis in Myocardial Infarction (TIMI)-IIIB Study. *J Am Coll Cardiol.* 1997;30:421-429.
7. Vaccarino RA, Johnson LL, Antunes ML, et al. Thallium-201 lung uptake and peak treadmill exercise first-pass ejection fraction. *Am Heart J.* 1995;129:320-329.
8. Manning F. Pulmonary thallium uptake: correlation with systolic and diastolic left ventricular function at rest and during exercise. *Am Heart J.* 1990;119:1137-1146.
9. Ilmer B, Reijs AE, Fioretti P, Reiber JH. Comparative study of three different approaches on the estimation of the lung-heart ratio in thallium 201 scintigrams in relation to the extent of coronary artery disease and left ventricular function. *Eur J Nucl Med.* 1991;18:252-258.
10. Giubbini R, Campini R, Milan E, et al. Evaluation of technetium-99m-sestamibi lung uptake: correlation with left ventricular function. *J Nucl Med.* 1995;36:58-63.
11. Hurwitz GA, Fox SP, Driedger AA, Willems C, Powe JE. Pulmonary uptake of sestamibi on early post-stress images: angiographic relationships, incidence and kinetics. *Nucl Med Commun.* 1993;14:15-22.
12. Hurwitz GA, Ghali SK, Husni M, et al. Pulmonary uptake of technetium-99m-sestamibi induced by dipyridamole-based stress or exercise. *J Nucl Med.* 1998;39:339-345.
13. Castellani M, Chiti A, Giovanella LC, Bestetti A, Lomuscio A, Tarolo GL. Thallium-201 lung uptake: comparison of an automatic and a manual method of ROI drawing. *J Nucl Biol Med.* 1993;37:213-217.
14. Berman DS, Kiat H, Friedman JD, et al. Separate acquisition rest thallium-201/stress technetium-99m sestamibi dual-isotope myocardial perfusion single-photon emission computed tomography: a clinical validation study. *J Am Coll Cardiol.* 1993;22:1455-1464.
15. Rozanski A, Diamond GA, Forrester JS, et al. Alternative referent standards for cardiac normality: implications for diagnostic testing. *Ann Intern Med.* 1984;101:164-171.
16. Friedman JD, Berman DS, Kiat H, et al. Rest and treadmill exercise first-pass radionuclide ventriculography: validation of left ventricular ejection fraction measurements. *J Nucl Cardiol.* 1994;1:382-388.
17. Germano G, Kiat H, Kavanagh PB, et al. Automatic quantification of ejection fraction from gated myocardial perfusion SPECT. *J Nucl Med.* 1995;36:2138-2147.
18. Palmas W, Friedman JD, Diamond GA, Silber H, Kiat H, Berman DS. Incremental value of simultaneous assessment of myocardial function and perfusion with technetium-99m sestamibi for prediction of extent of coronary artery disease. *J Am Coll Cardiol.* 1995;25:1024-1031.
19. Benari B, Kiat H, Erel J, et al. Repeatability of treadmill exercise ejection fraction and wall motion using technetium 99m-labeled sestamibi first-pass radionuclide ventriculography. *J Nucl Cardiol.* 1995;2:478-484.
20. Berman DS, Hachamovitch R, Kiat H, et al. Incremental value of prognostic testing in patients with known or suspected ischemic heart disease: a basis for optimal utilization of exercise technetium-99m sestamibi myocardial perfusion single-photon emission computed tomography. *J Am Coll Cardiol.* 1995;26:639-647.
21. Mazzanti M, Germano G, Kiat H, et al. Identification of severe and extensive coronary artery disease by automatic measurement of transient ischemic dilation of the left ventricle in dual-isotope myocardial perfusion SPECT. *J Am Coll Cardiol.* 1996;27:1612-1620.
22. Germano G, Kavanagh PB, Chen J, et al. Operator-less processing of myocardial perfusion SPECT studies. *J Nucl Med.* 1995;36:2127-2132.
23. Liu P, Kiess M, Okada RD, et al. Increased thallium lung uptake after exercise in isolated left anterior descending coronary artery disease. *Am J Cardiol.* 1985;55:1469-1473.
24. Ilmer B, Reijs AE, Reiber JH, Bakker W, Fioretti P. Relationships between the lung-heart ratio assessed from post-exercise thallium-201 myocardial tomograms, myocardial ischemia and the extent of coronary artery disease. *Int J Card Imaging.* 1990;6:135-141.
25. Nishimura S, Mahmarian JJ, Verani MS. Significance of increased lung thallium uptake during adenosine thallium-201 scintigraphy. *J Nucl Med.* 1992;33:1600-1607.
26. Manning F. A new method for quantification of pulmonary thallium uptake in myocardial SPECT studies. *Eur J Nucl Med.* 1990;16:213-222.
27. Saha M, Farrand TF, Brown KA. Lung uptake of technetium 99m sestamibi: relation to clinical, exercise, hemodynamic, and left ventricular function variables. *J Nucl Cardiol.* 1994;1:52-56.
28. Martinez EE, Horowitz SF, Castello HJ, et al. Lung and myocardial thallium-201 kinetics in resting patients with congestive heart failure: correlation with pulmonary capillary wedge pressure. *Am Heart J.* 1992;123:427-432.
29. Papadopoulos CL, Doumas AS, Koliakos G, Gitsios C, Sakadamis G. Increased lung uptake during myocardial scintigraphy improves the detection and localization of coronary artery disease. *Angiology.* 1995;46:1015-1020.
30. Hurwitz GA, MacDonald AC. Critical stenoses of the left anterior descending artery: predominant role in stress-induced pulmonary uptake of ²⁰¹thallium. *Can J Cardiol.* 1994;10:982-988.
31. Hansen CL, Sangrigoli R, Nkadi E, Kramer M. Comparison of pulmonary uptake with transient cavity dilation after exercise thallium-201 perfusion imaging. *J Am Coll Cardiol.* 1999;33:1323-1327.
32. Johnson LL, Verdesca SA, Aude WY, et al. Postischemic stunning can affect left ventricular ejection fraction and regional wall motion on post-stress gated sestamibi tomograms. *J Am Coll Cardiol.* 1997;30:1641-1648.
33. Gill JB, Ruddy TD, Newell JB, Finkelstein DM, Strauss HW, Boucher CA. Prognostic importance of thallium uptake by the lungs during exercise in coronary artery disease. *N Engl J Med.* 1987;317:1486-1489.